Supporting Information

Rare-earth/zinc heterometallic complexes containing both alkoxy-amino-bis(phenolato) and chiral salen ligands: synthesis and catalytic application for copolymerization of CO_2 with cyclohexene oxide

Ruoyu Xu, Linyan Hua, Li Xiang, Yingming Yao, Xuebing Leng and Yaofeng Chen

Contents

Table S1 Crystallographic Data and Refinement for the complexes.

	Y-(*R*,*R*)Zn·benzene	Dy-(*R*,*R*)Zn·toluene	Sm-(*R*,*R*)Zn·benzene
formula	$C_{65}H_{95}N_4O_5Si_2YZn$	$C_{66}H_{97}N_4O_5Si_2DyZn$	$C_{65}H_{95}N_4O_5Si_2SmZn$
fw	1222.90	1310.52	1284.34
color	colorless	colorless	colorless
cryst syst.	monoclinic	monoclinic	monoclinic
space group	$P2_1$	$P2_1$	$P2_1$
a, Å	10.3789(3)	10.4278(2)	10.3709(2)
b, Å	25.7640(7)	25.8777(4)	26.0470(5)
c, Å	15.3261(4)	15.2743(2)	15.2688(3)
α, deg	90	90	90
β, deg	108.3420(10)	108.6460(8)	108.6854(10)
γ, deg	90	90	90
V, Å^3	3890.02(19)	3905.39(11)	3907.18(13)
Z	2	2	2
D_{calcd}, (mg/m^3)	1.044	1.114	1.092
F(000)	1300	1370	1346
T(K)	170	170	170
θ range, deg	2.984, 54.926	5.318, 54.948	3.915, 54.889
no. of refns collected	41757	38609	40043
no. of unique refns	14566	13053	10719
no. of obsd refns ($I > 2\sigma(I)$)	11687	12128	10068
No. of params	723	721	711
Final R, R_w (I > 2σ(I))	0.0557, 0.1305	0.0620, 0.1772	0.0412, 0.1043
Goodness-of-fit on F^2	1.008	1.055	1.027
$\Delta\rho_{max, min}$, eÅ^{-3}	0.655, -1.007	1.163, -0.840	0.855, -1.080

	La-(*R*,*R*)Zn·toluene	Sm-(*S*,*S*)Zn ·toluene
formula	$C_{66}H_{97}N_4O_5Si_2LaZn$	$C_{66}H_{97}N_4O_5Si_2SmZn$
fw	1286.93	1298.37
color	colorless	colorless
cryst syst.	monoclinic	monoclinic
space group	$P2_1$	$P2_1$
a, Å	10.3888(2)	10.3825(2)
b, Å	26.3263(5)	26.0638(5)
c, Å	15.2186(3)	15.2519(3)
α, deg	90	90
β, deg	108.8760(10)	108.7512(9)
γ, deg	90	90
V, $Å^3$	3938.42(13)	3908.21(13)
Z	2	2
D_{calcd}, (mg/m^3)	1.085	1.103
F(000)	1352	1362
T(K)	170	173
θ range, deg	3.960, 54.930	3.962, 55.011
no. of refns collected	38434	39799
no. of unique refns	12711	12221
no. of obsd refns ($I > 2\sigma(I)$)	12348	11980
No. of params	733	721
Final R, R_w ($I > 2\sigma(I)$)	0.0565, 0.1501	0.0356, 0.0959
Goodness-of-fit on F^2	1.026	1.030
$\Delta\rho_{max, min}$, $eÅ^{-3}$	1.110, -0.756	0.969, -0.461

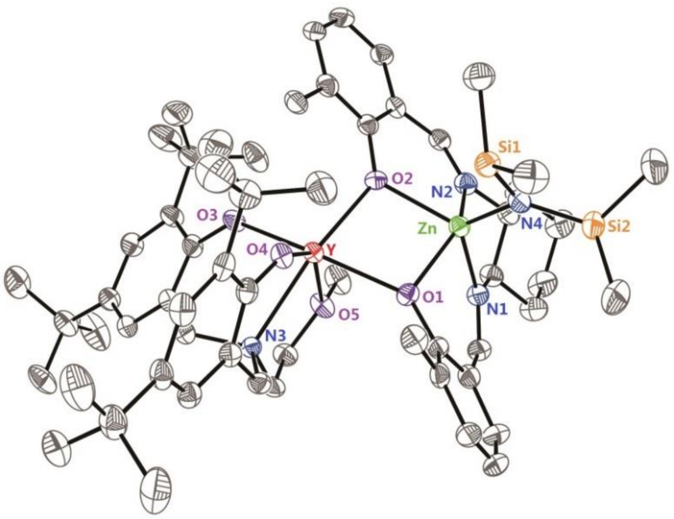

Figure S1. Molecular structure of complex Y-(*R*,*R*)Zn with thermal ellipsoids at the 30% probability level. Hydrogen atoms of the complex and benzene molecule in the lattice were omitted for clarity. Selected distances [Å] and angles [°]: Y−O1 2.262(4), Y−O2 2.273(4), Y−O3 2.151(4), Y−O4 2.131(4), Y−O5 2.446(4), Y−N3 2.485(5), Zn−O1 2.163(4), Zn−O2 2.135(4), Zn−N1 2.109(5), Zn−N2 2.094(6), Zn−N4 1.932(6), Y···Zn 3.413(1); O1−Y−O2 75.9(2), O1−Zn−O2 80.9(2), Zn1−O−Y1 100.9(2), Zn−O2−Y 101.1(2), O3−Y−O4 100.7(2), O4−Y−O5 146.1(2)°.

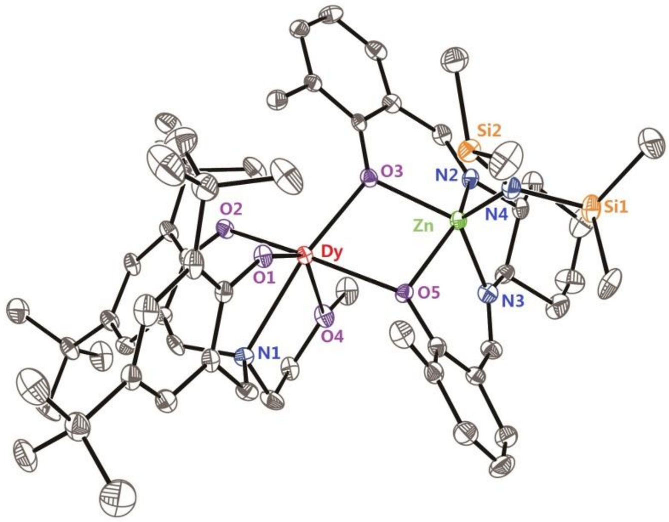

Figure S2. Molecular structure of complex Dy-(*R*,*R*)Zn with thermal ellipsoids at the 30% probability level. Hydrogen atoms of the complex and toluene molecule in the lattice were omitted for clarity. Selected distances [Å] and angles [°]: Dy–O1 2.148(7), Dy–O2 2.157(7), Dy–O3 2.293(7), Dy–O5 2.266(7), Dy–O4 2.467(8), Dy–N1 2.499(9), Zn–O3 2.125(7), Zn–O5 2.169(7), Zn–N2 2.107(10), Zn–N3 2.101(10), Zn–N4 1.932(10), Dy···Zn 3.419(2); O3–Dy–O5 75.8(2), O3–Zn–O5 81.4(3), Zn–O3–Dy 101.4(3), Zn–O5–Dy 100.8(3), O–Dy–O 100.8(3), O–Dy–O 145.0(3)°.

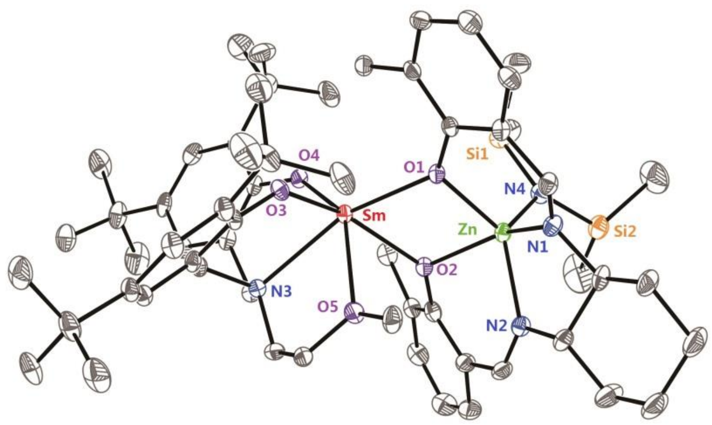

Figure S3. Molecular structure of complex Sm-(*S*,*S*)Zn with thermal ellipsoids at the 30% probability level. Hydrogen atoms of the complex and toluene molecule in the lattice were omitted for clarity. Selected distances [Å] and angles [°]: Sm–O1 2.348(4), Sm–O2 2.369(4), Sm–O3 2.199(4), Sm–O4 2.149(4), Sm–O5 2.537(4), Sm–N3 2.560(5), Zn–O1 2.154(4), Zn–O2 2.124(4), Zn–N1 2.107(5), Zn–N2 2.115(5), Zn–N4 1.943(6), Sm···Zn 3.487(1); O1–Sm–O2 73.6(1), O1–Zn–O2 82.7(1), Zn–O1–Sm 101.5(2), Zn–O2–Sm 101.8(2), O3–Sm–O4 102.2(2), O4–Sm–O5 142.7(2)°.

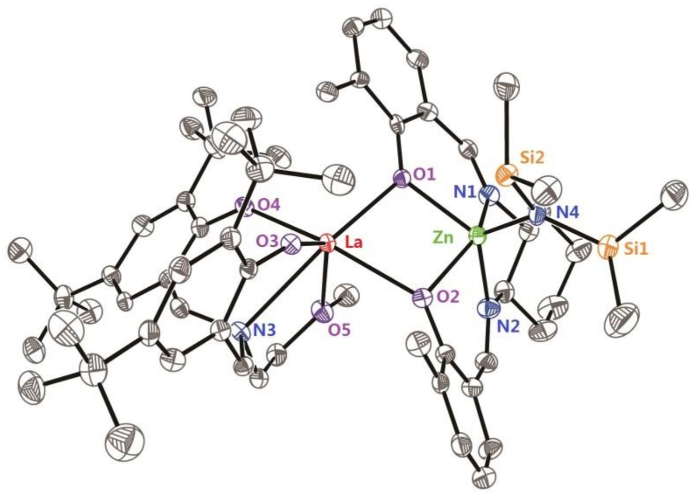

Figure S4. Molecular structure of complex La-(*R*,*R*)Zn with thermal ellipsoids at the 30% probability level. Hydrogen atoms of the complex and toluene molecule in the lattice were omitted for clarity. Selected distances [Å] and angles [°]: La–O1 2.440(6), La–O2 2.404(6), La–O3 2.252(6), La–O4 2.286(6), La–O5 2.595(7), La–N3 2.703(7), Zn–O1 2.121(6), Zn–O2 2.155(6), Zn–N1 2.109(8), Zn–N2 2.116(9), Zn–N4 1.952(8), La···Zn 3.530(1); O1–La–O2 72.8(2), O1–Zn–O2 84.5(2), Zn–O1–La 101.2(2), Zn–O2–La 101.3(2), O3–La–O4 100.2(2), O3–La–O5 137.0(2)°.

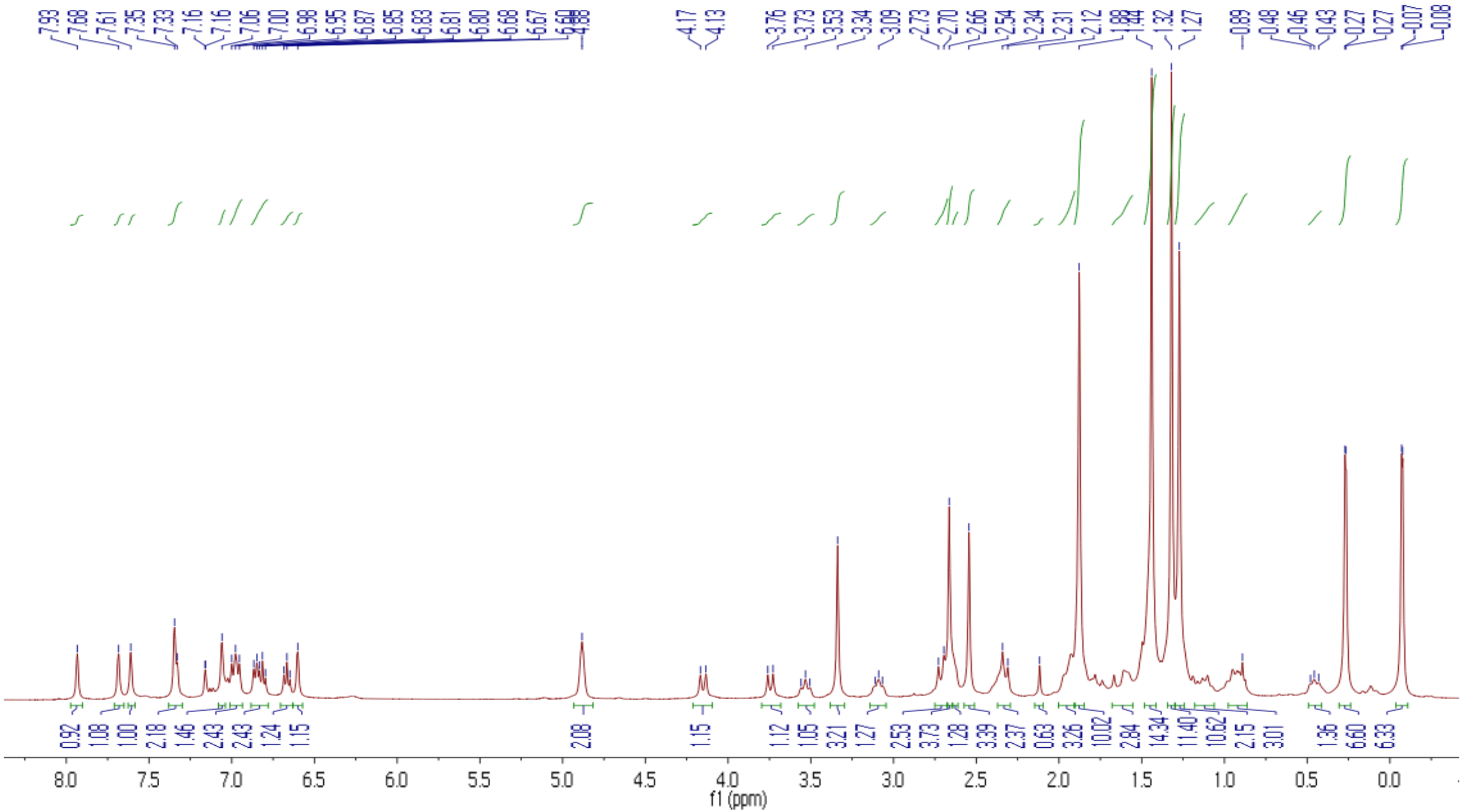

Figure S5. ^{1}H NMR spectrum of Y-(*R*,*R*)Zn (400 MHz, C_6D_6, 25 ºC).

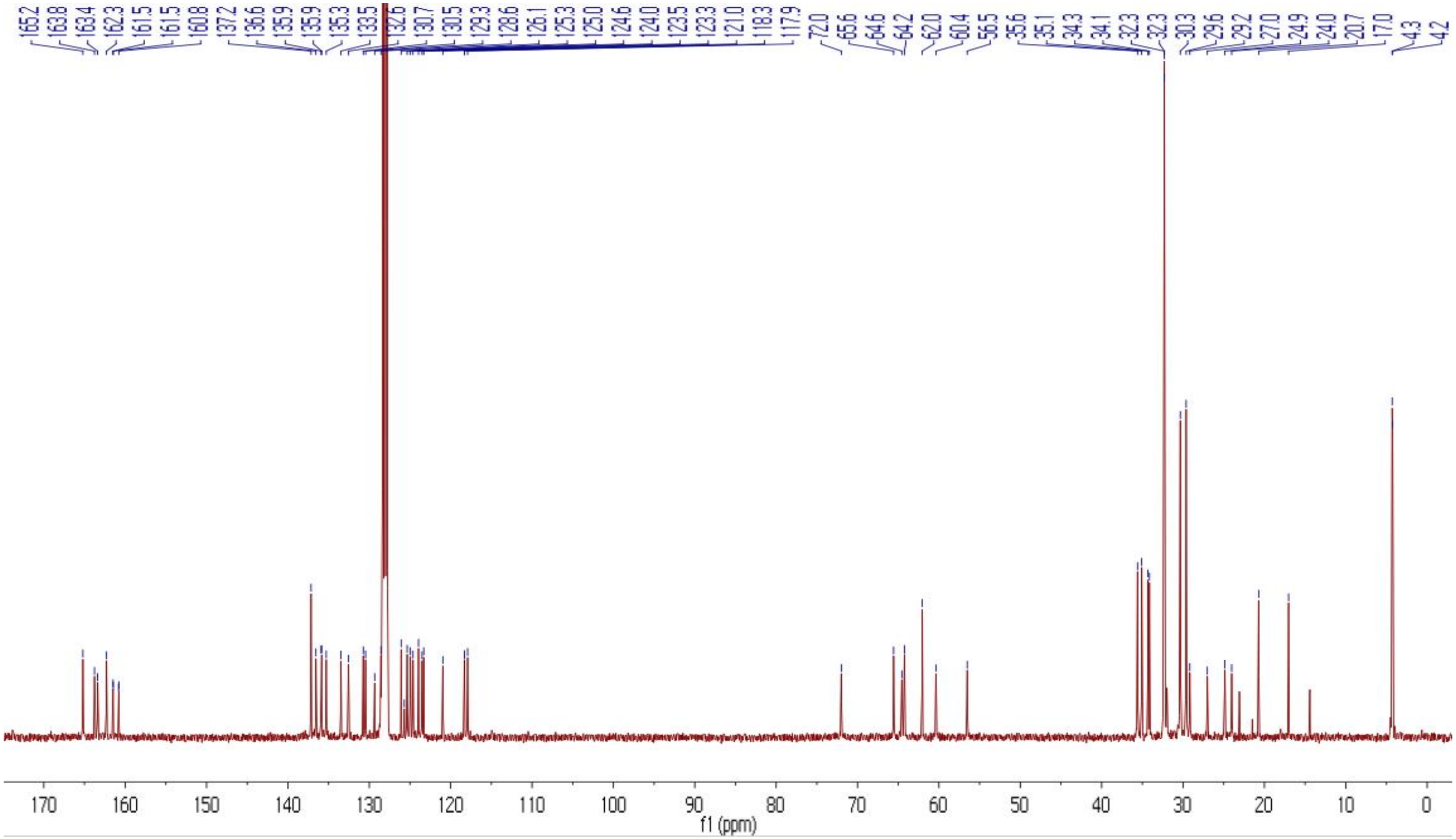

Figure S6. $^{13}C\{^{1}H\}$ NMR spectrum of Y-(*R*,*R*)Zn (100 MHz, C_6D_6, 25 °C).

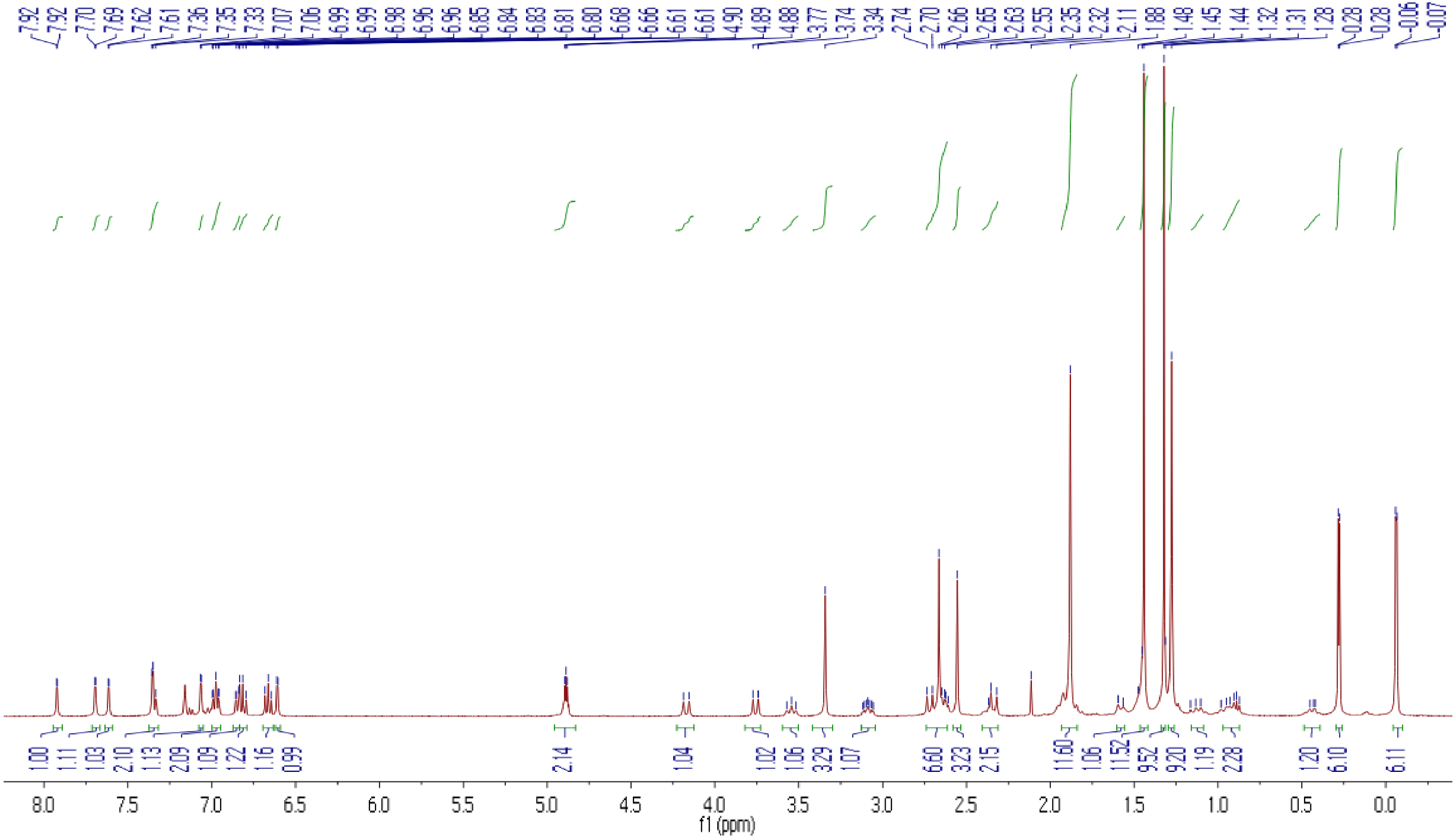

Figure S7. ^{1}H NMR spectrum of Y-(*S*,*S*)Zn (400 MHz, C_6D_6, 25 ºC).

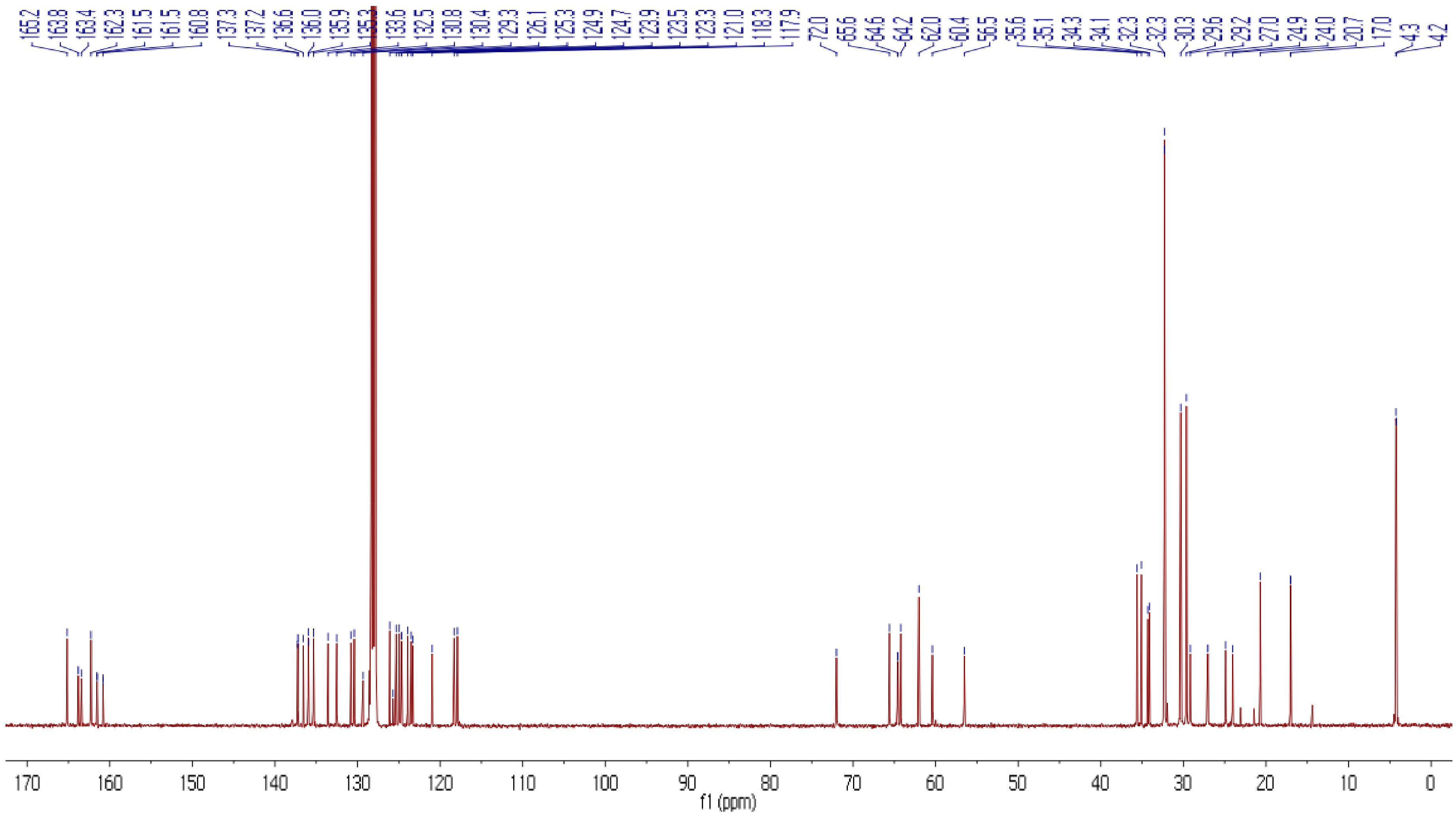

Figure S8. $^{13}C\{^1H\}$ NMR spectrum of Y-(*S*,*S*)Zn (100 MHz, C_6D_6, 25 ^oC).

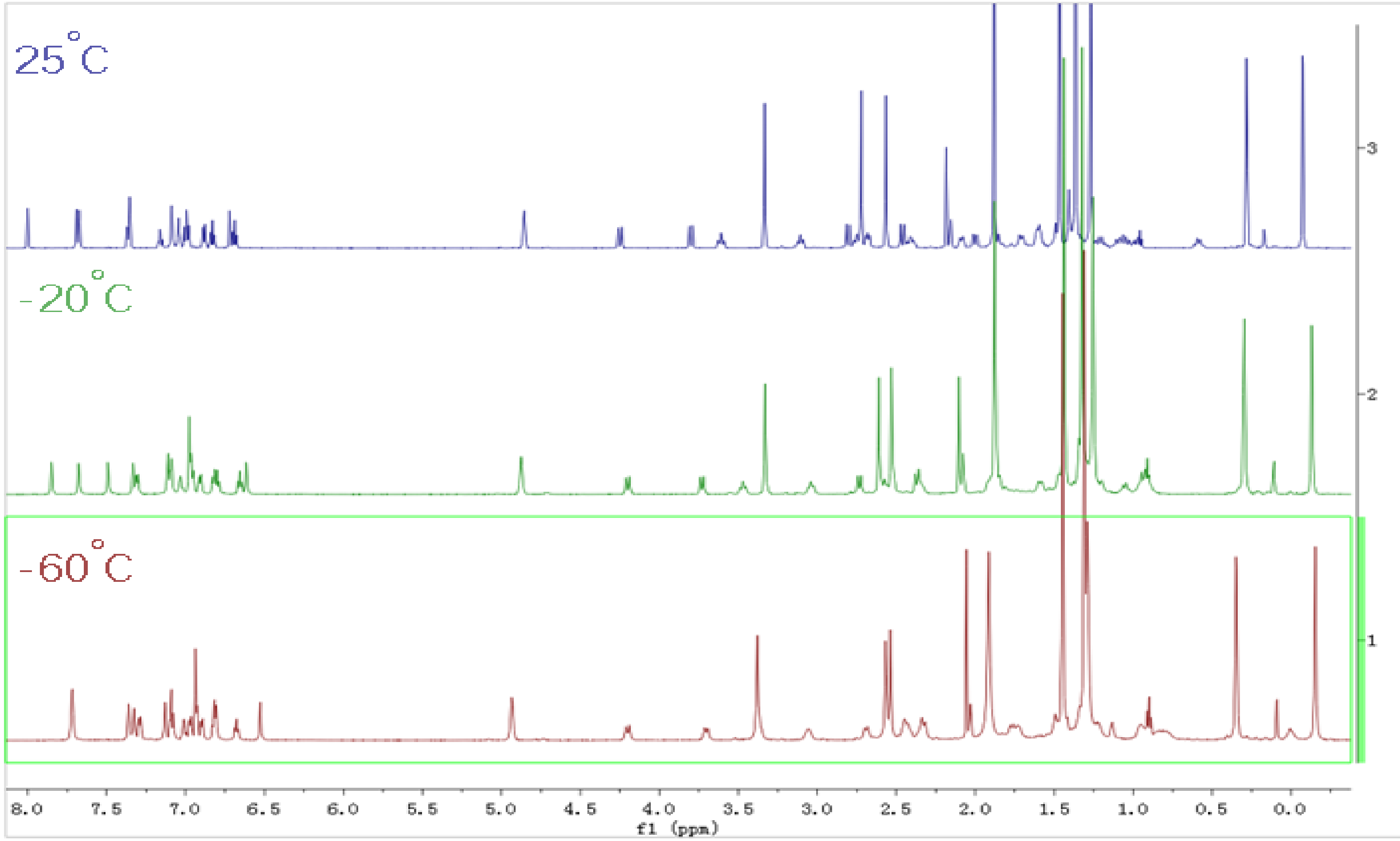

Figure S9. Variable temperature ^{1}H NMR spectra of Y-(*S*,*S*)Zn (600 MHz, toluene-d_8).

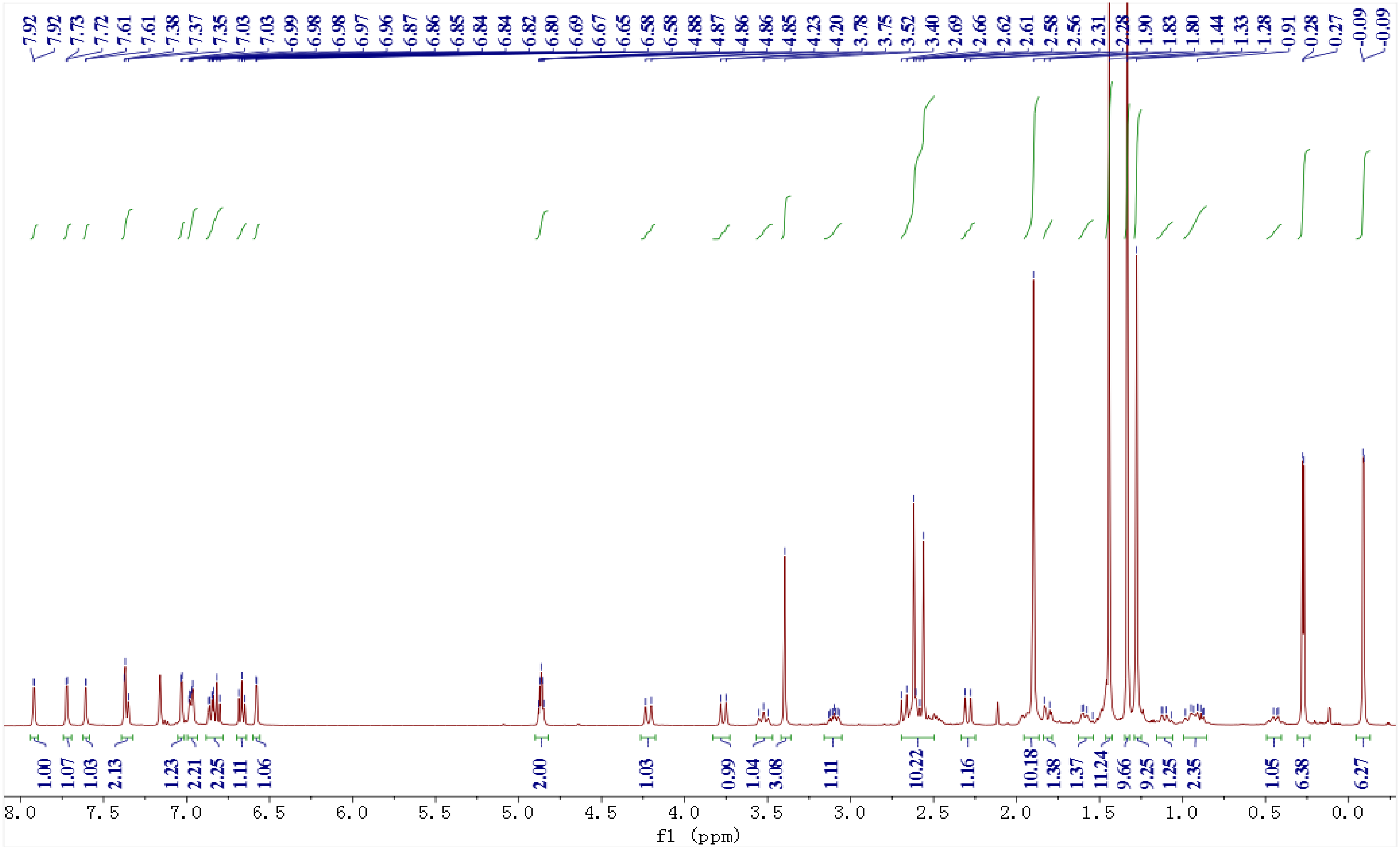

Figure S10. [1]H NMR spectrum of Lu-(*R*,*R*)Zn (400 MHz, C_6D_6, 25 ºC).

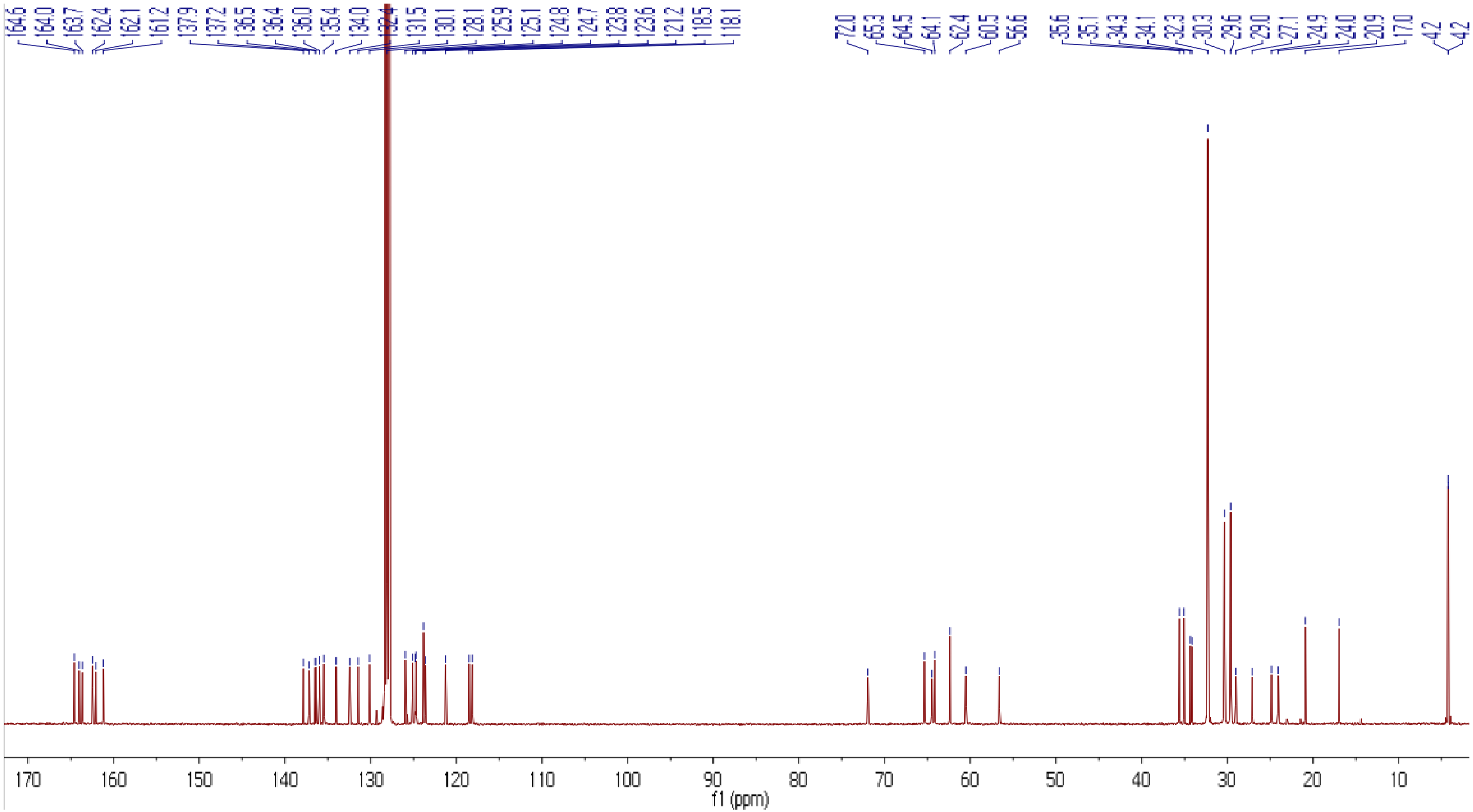

Figure S11. $^{13}C\{^{1}H\}$ NMR spectrum of Lu-(*R*,*R*)Zn (100 MHz, C_6D_6, 25 ºC).

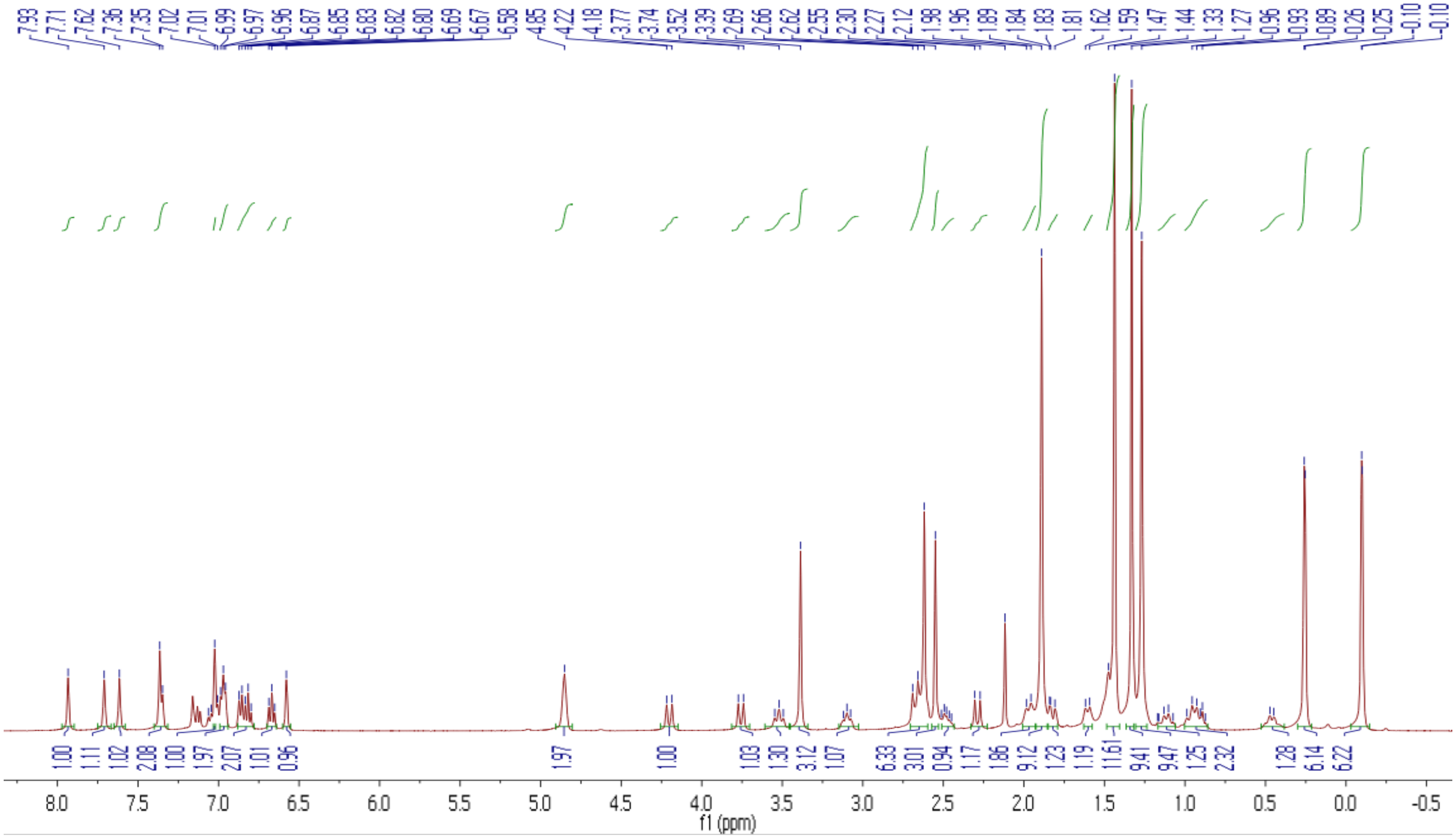

Figure S12. ^{1}H NMR spectrum of Lu-(*S*,*S*)Zn (400 MHz, C_6D_6, 25 °C).

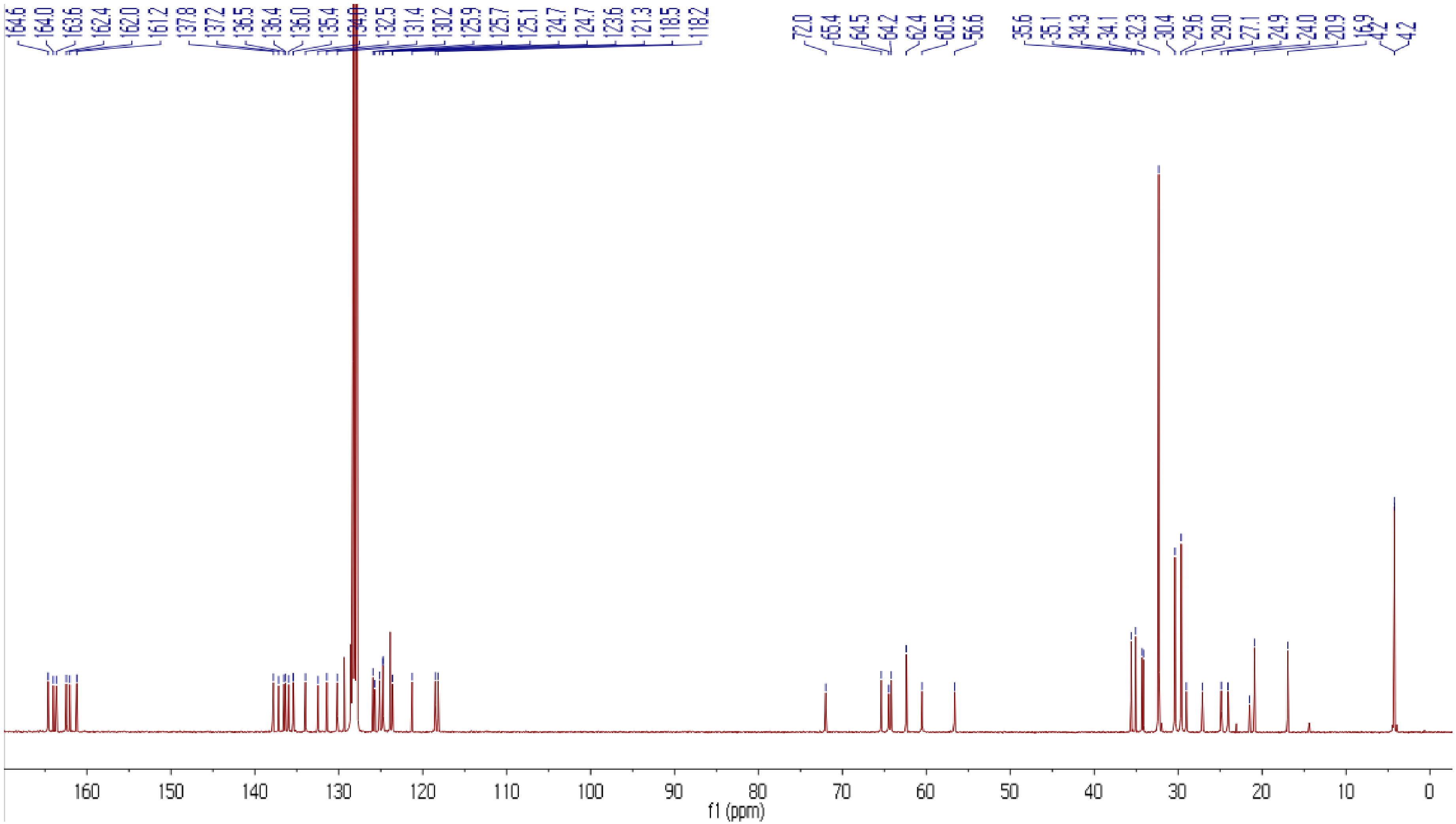

Figure S13. $^{13}C\{^{1}H\}$ NMR spectrum of Lu-(*S*,*S*)Zn (100 MHz, C_6D_6, 25 ºC).

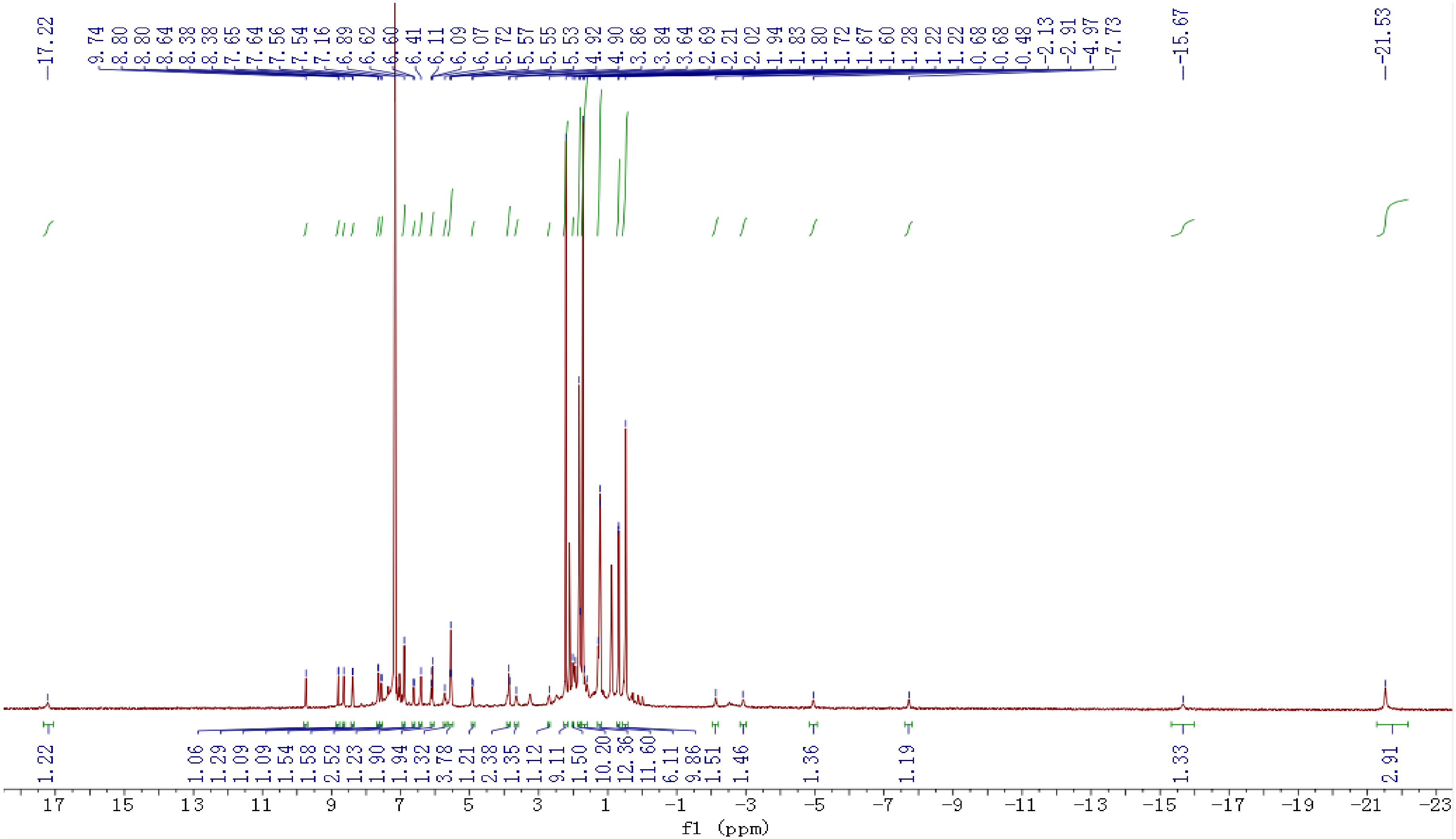

Figure S14. [1]H NMR spectrum of Sm-(*R*,*R*)Zn (400 MHz, C_6D_6, 25 °C).

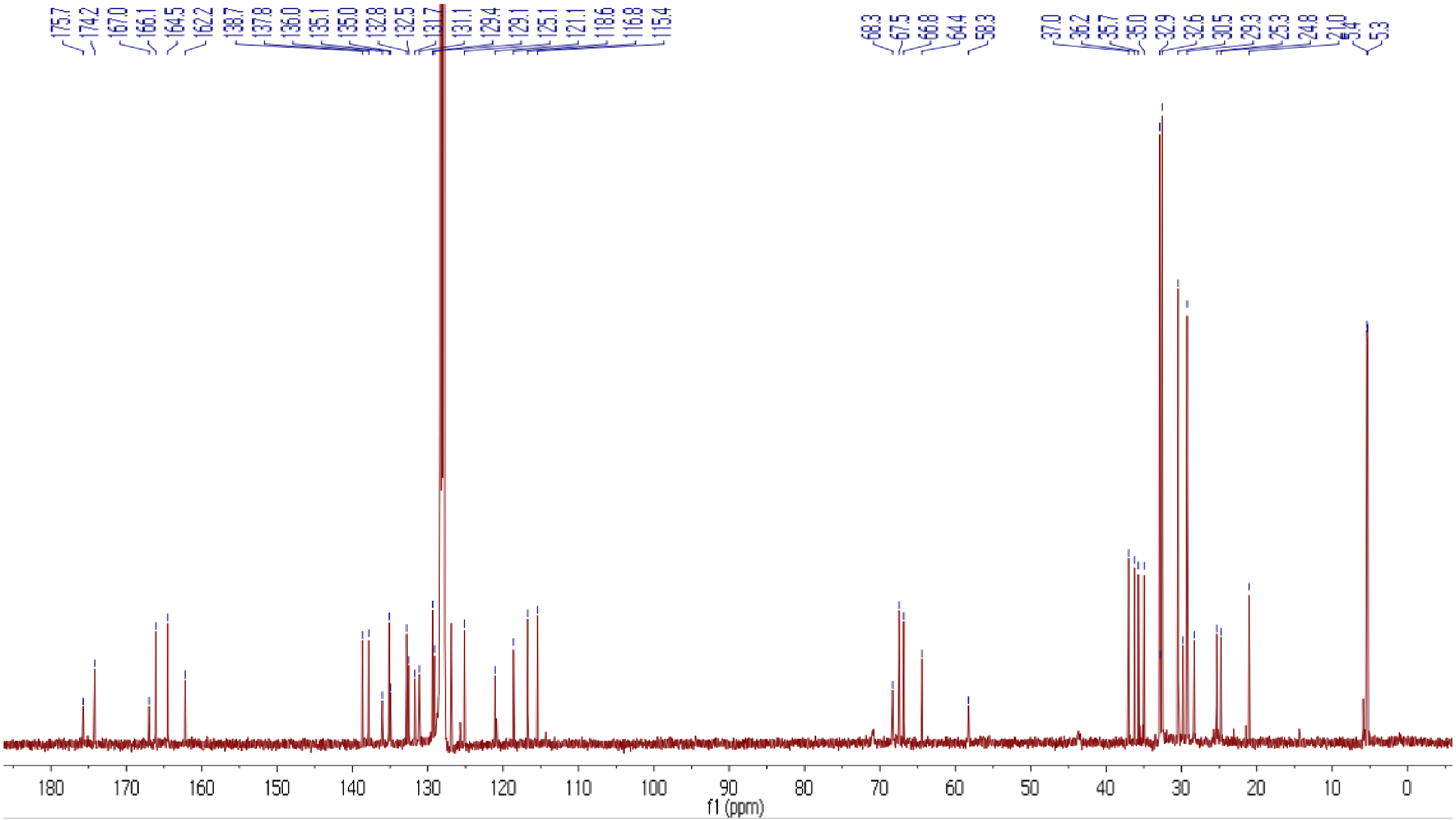

Figure S15. $^{13}C\{^{1}H\}$ NMR spectrum of Sm-(*R*,*R*)Zn (100 MHz, C_6D_6, 25 °C).

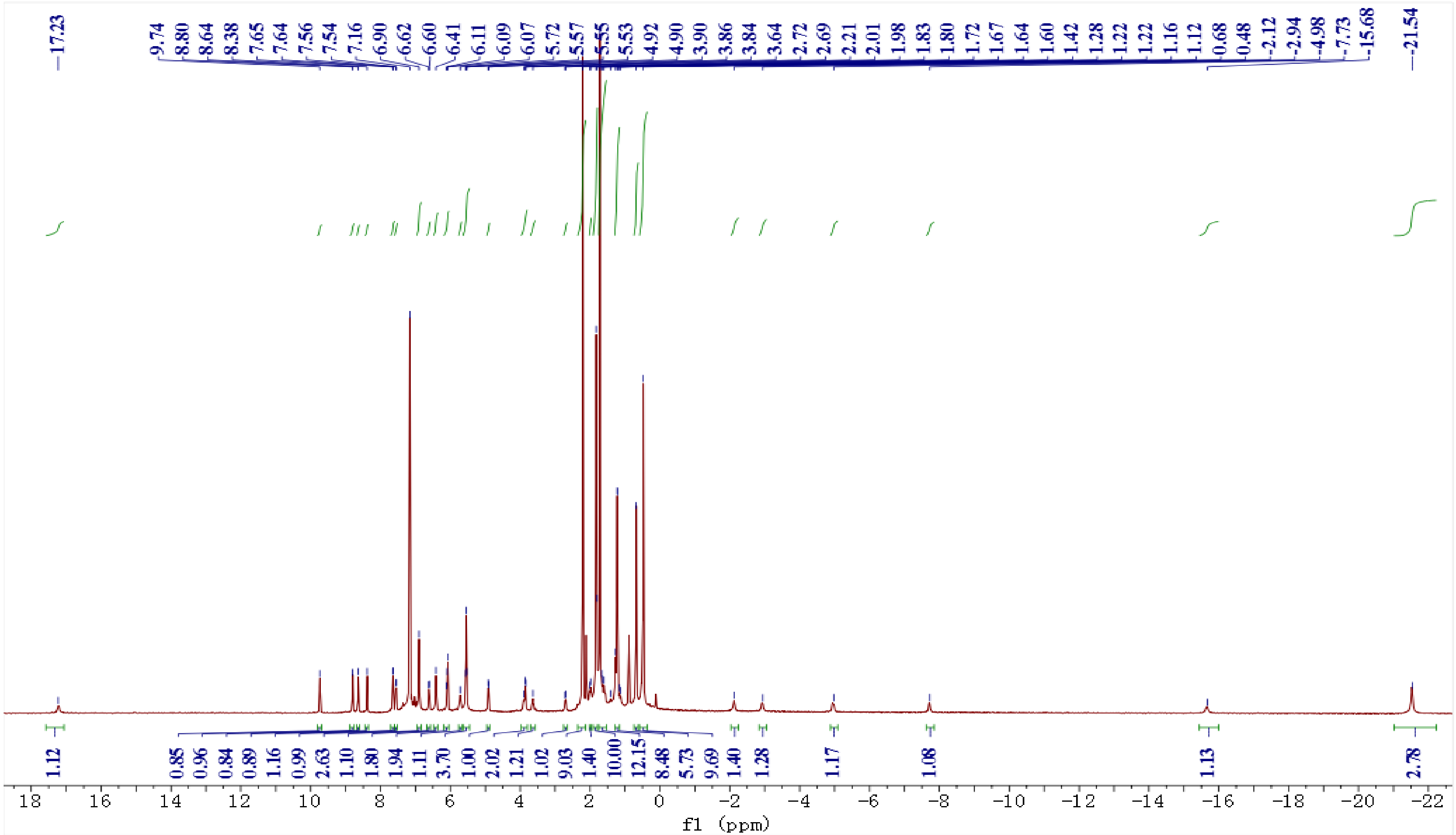

Figure S16. ^{1}H NMR spectrum of Sm-(*S*,*S*)Zn (400 MHz, C_6D_6, 25 ^{o}C).

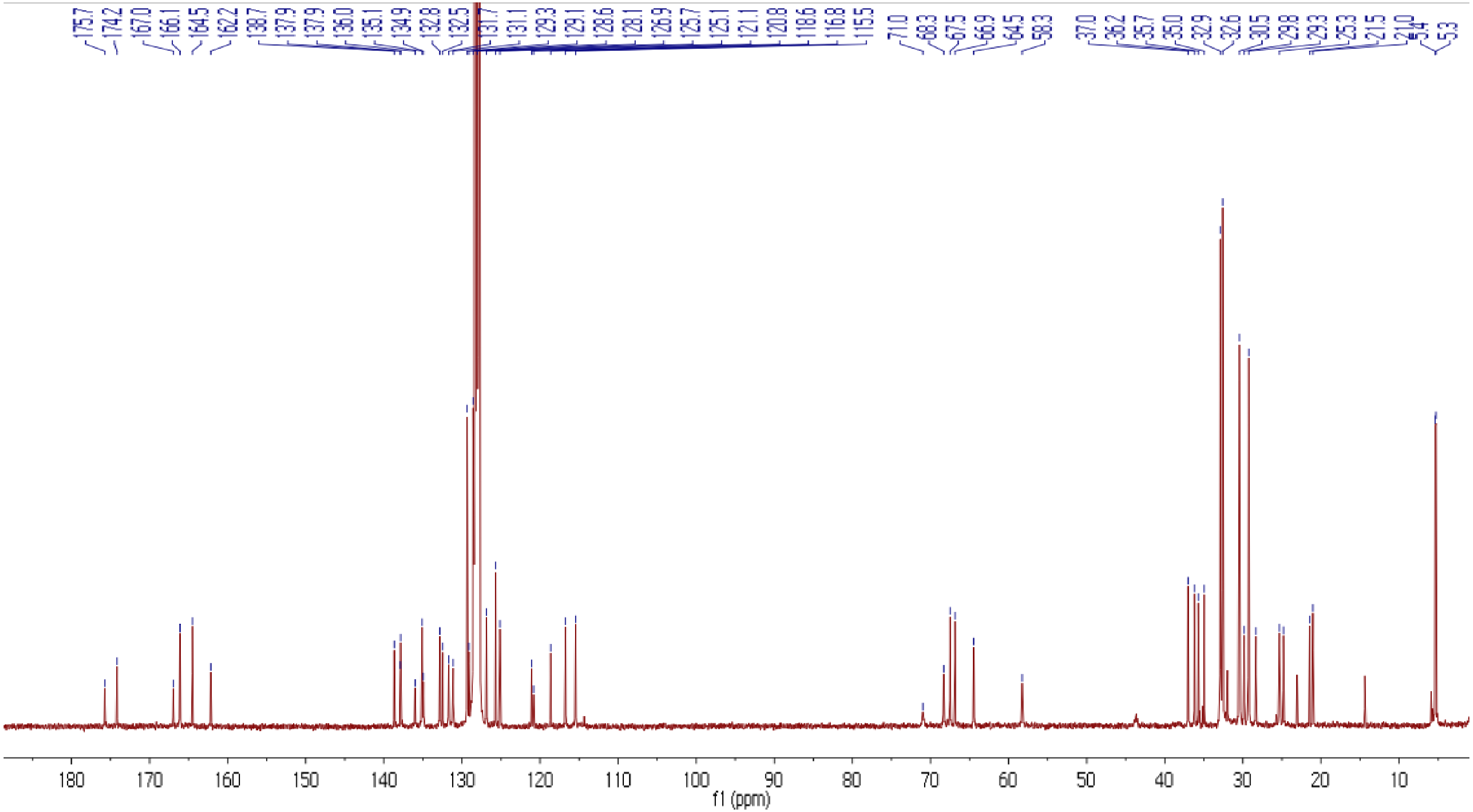

Figure S17. $^{13}C\{^{1}H\}$ NMR spectrum of Sm-(*S*,*S*)Zn (100 MHz, C_6D_6, 25 ºC).

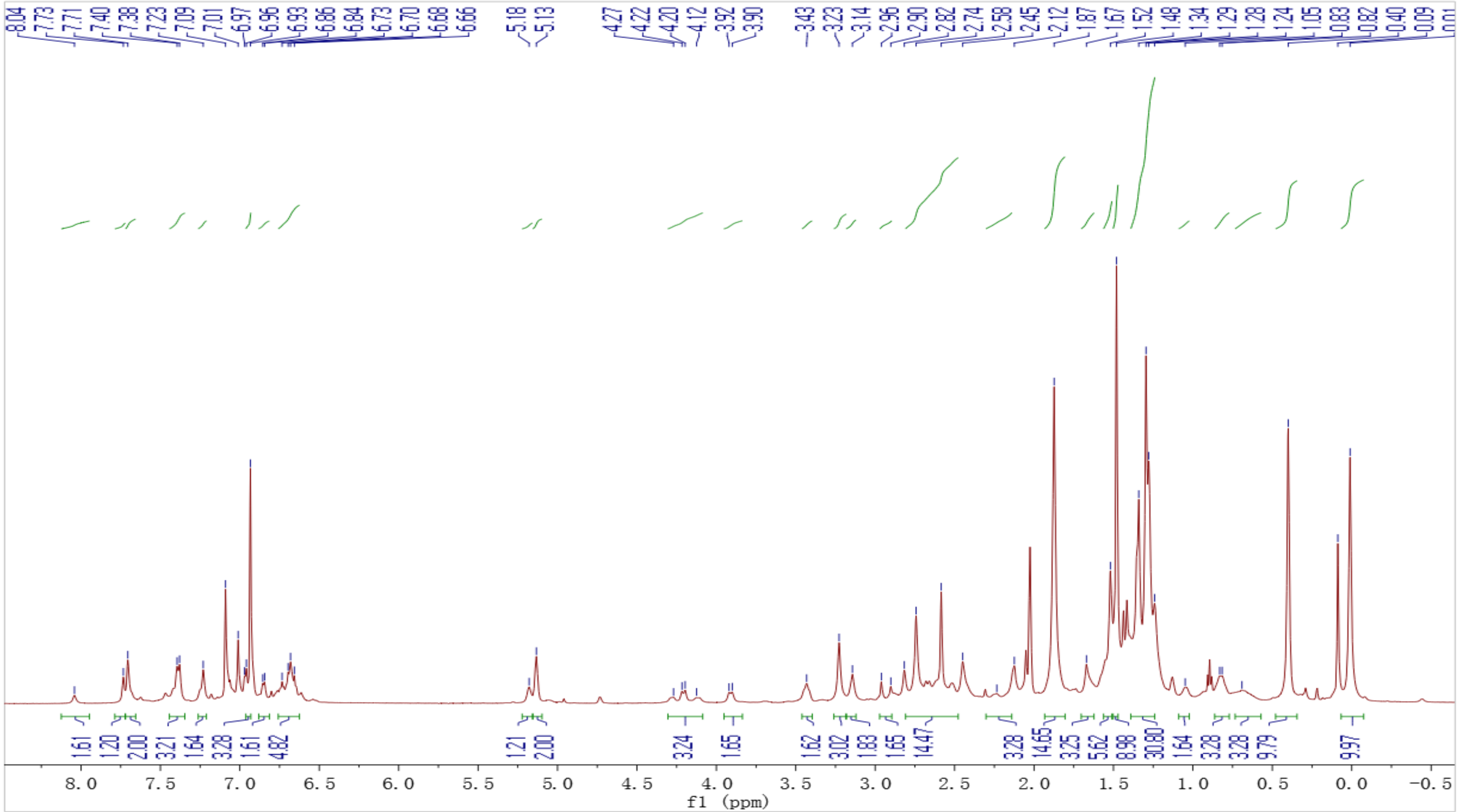

Figure S18. ^{1}H NMR spectrum of La-(*R*,*R*)Zn (600 MHz, toluene-d_8, -60 ^{o}C)

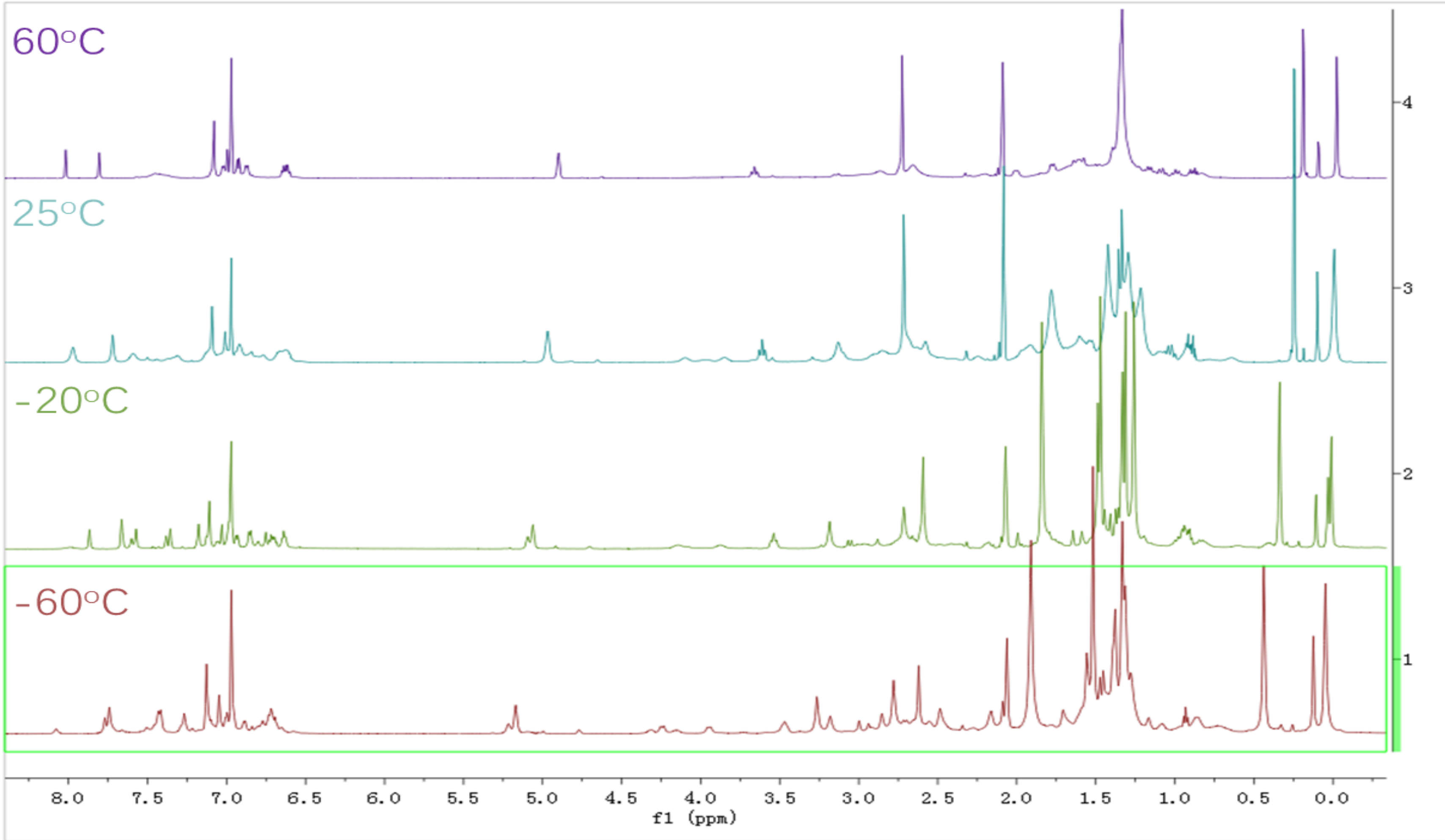

Figure S19. Variable temperature [1]H NMR spectra of La-(*R*,*R*)Zn (600 MHz, toluene-d_8)

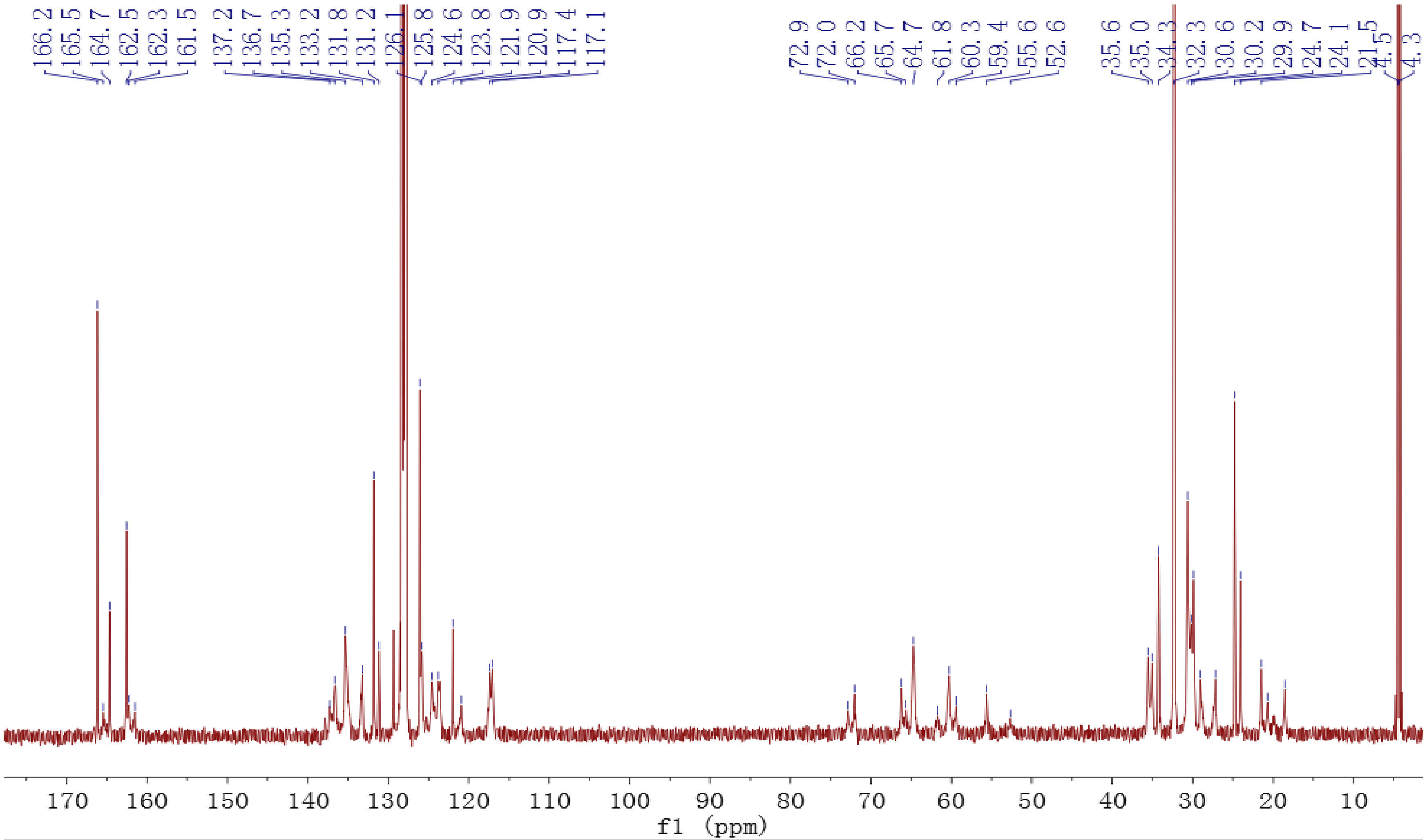

Figure S20. $^{13}C\{^{1}H\}$ NMR spectrum of La-(*R*,*R*)Zn (100 MHz, C_6D_6, 25 ºC).

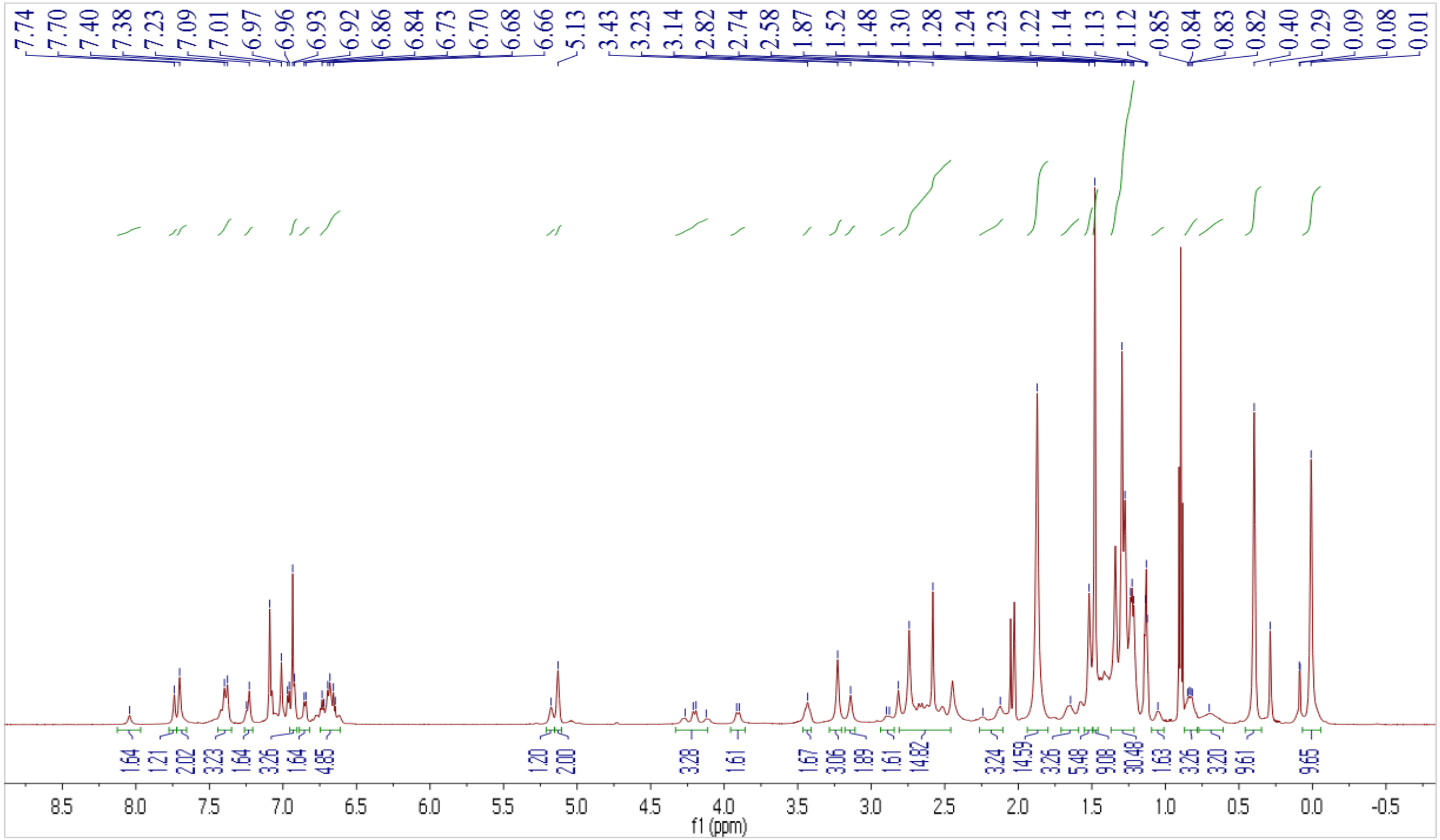

Figure S21. ^{1}H NMR spectrum of La-(*S*,*S*)Zn (600 MHz, toluene-d_8, -60 ^{o}C).

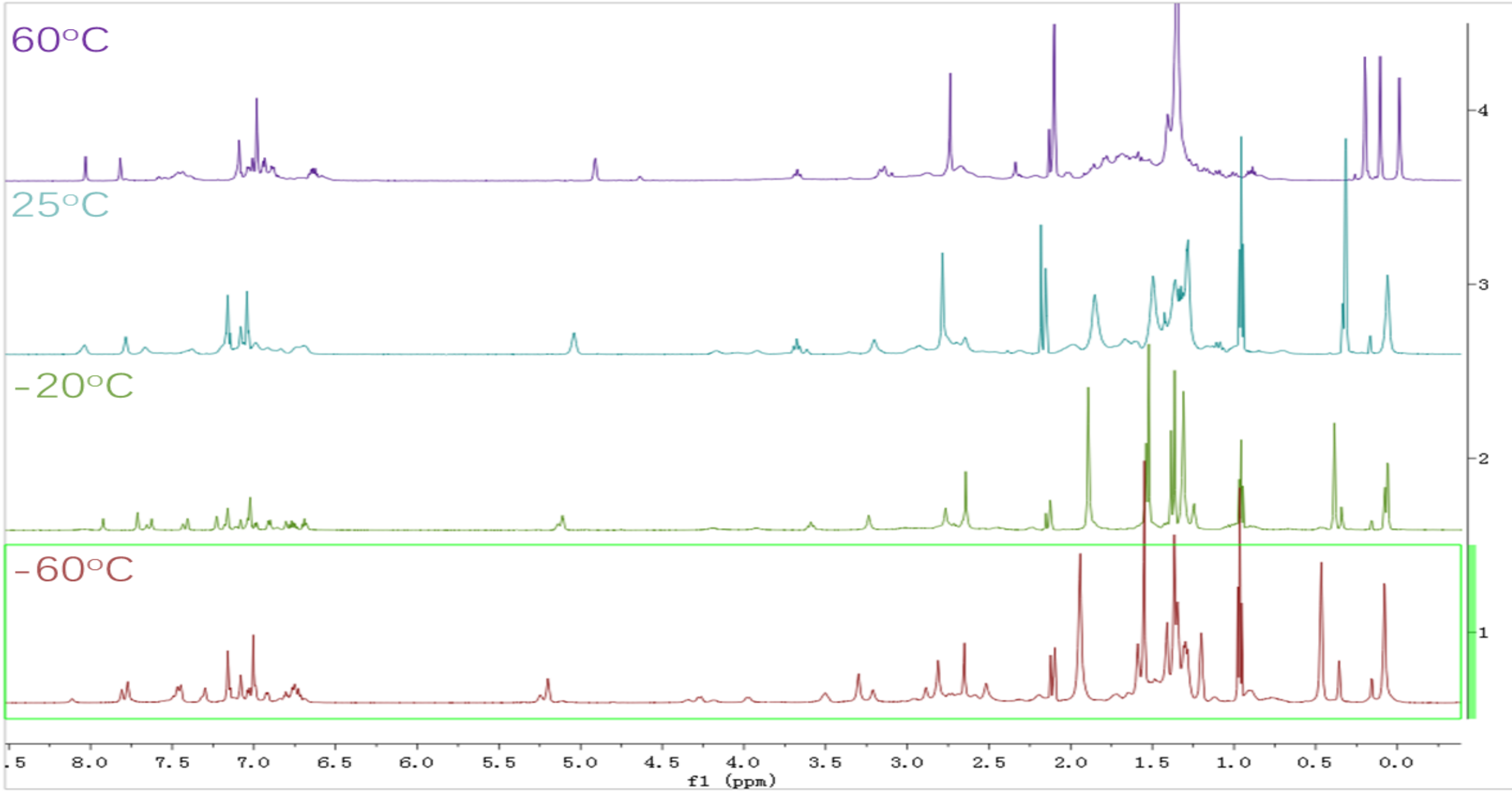

Figure S22. Variable temperature ^{1}H NMR spectrum of La-(*S*,*S*)Zn**,** (600 MHz, toluene-d_8. From the bottom to the top: 60, 25, -20, -60 °C)

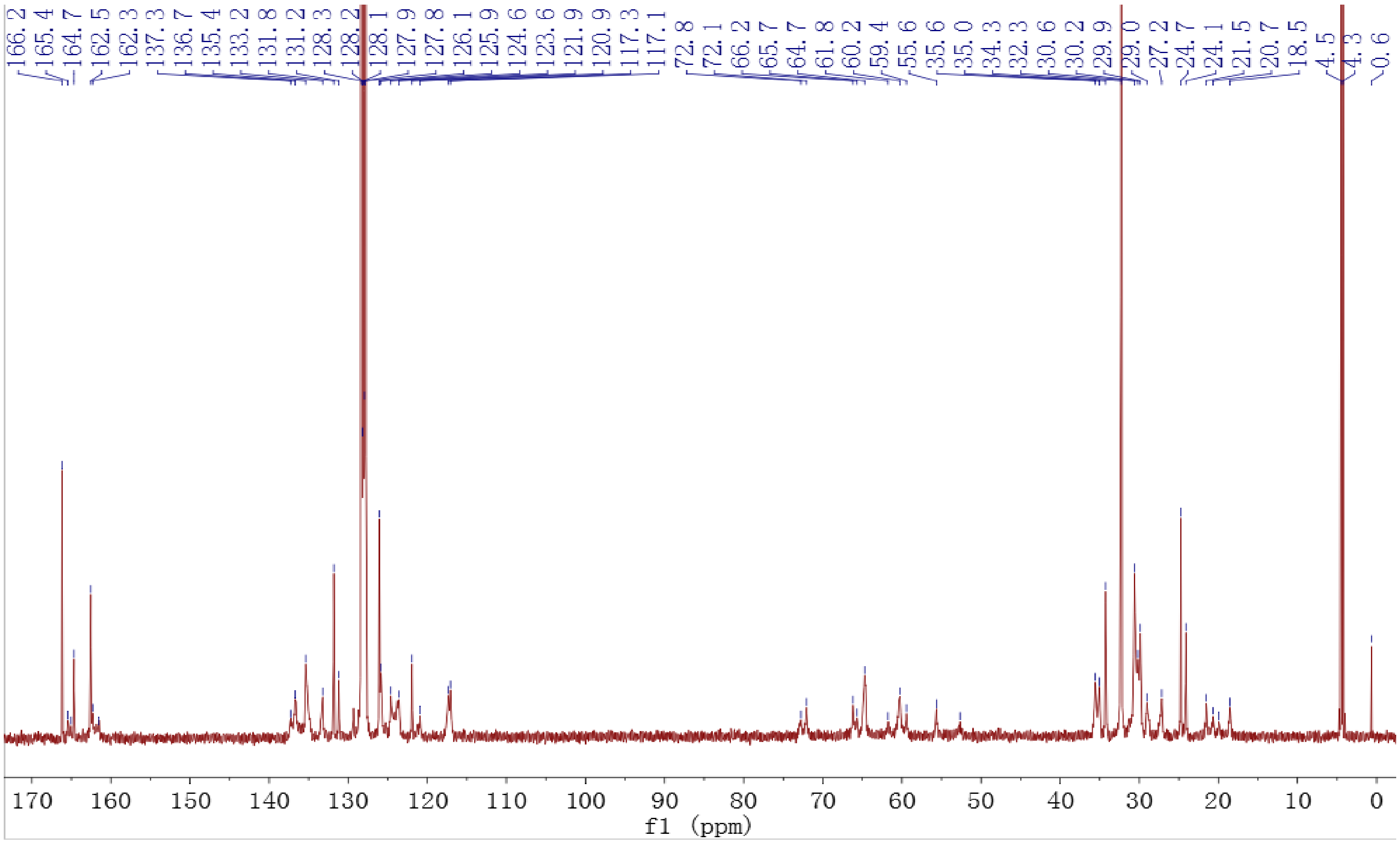

Figure S23. $^{13}C\{^{1}H\}$ NMR spectrum of La-(*S*,*S*)Zn (100 MHz, C_6D_6, 25 °C).

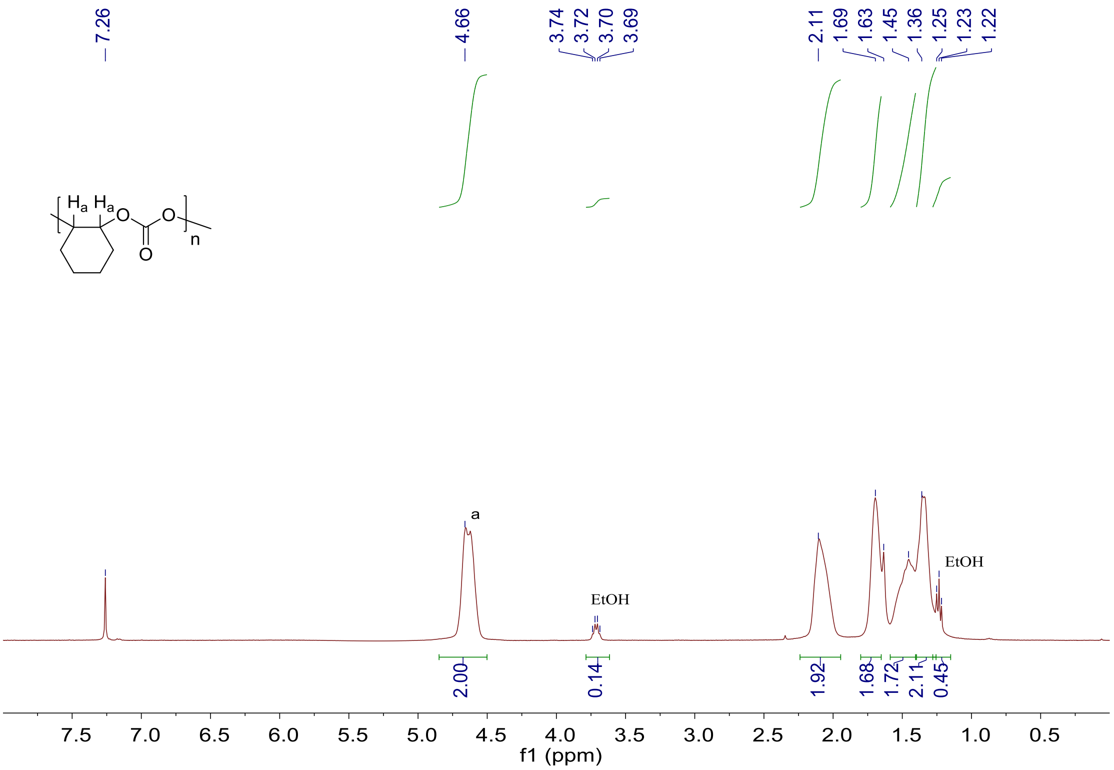

Figure S24 ^{1}H NMR spectra of the poly(cyclohexene carbonate) (Table 1, entry 10) (400 MHz, $CDCl_3$, 25 °C).

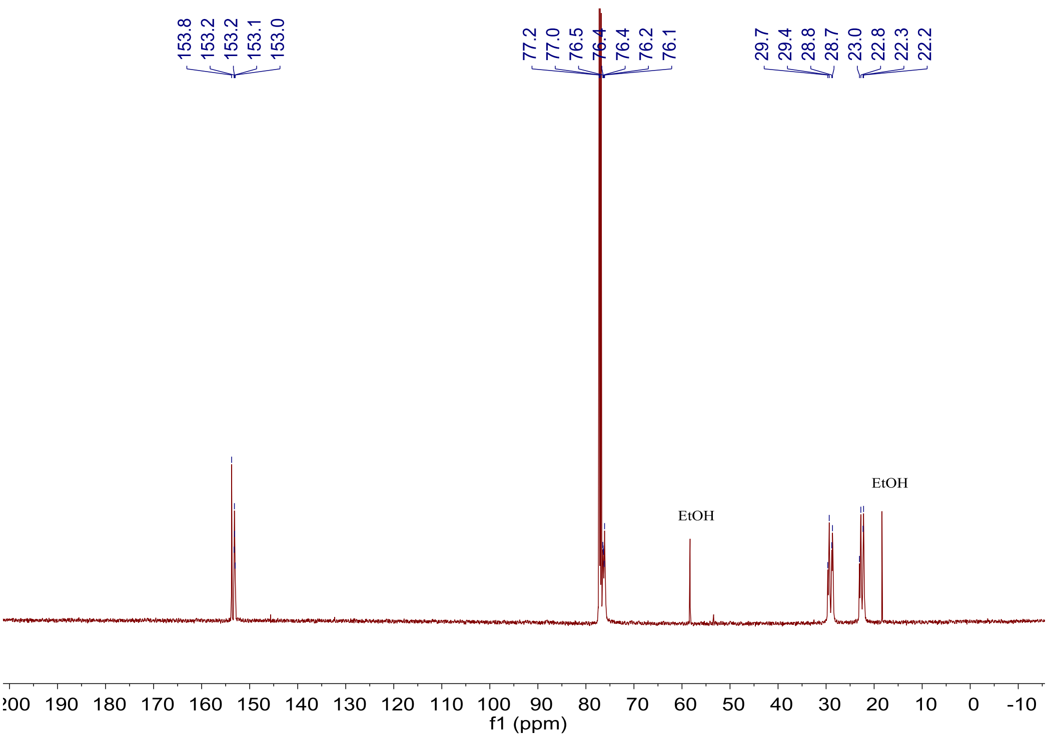

Figure S25 $^{13}C\{^{1}H\}$ NMR spectrum of the poly(cyclohexene carbonate) (Table 1, entry 10) (400 MHz, $CDCl_3$, 25 °C).

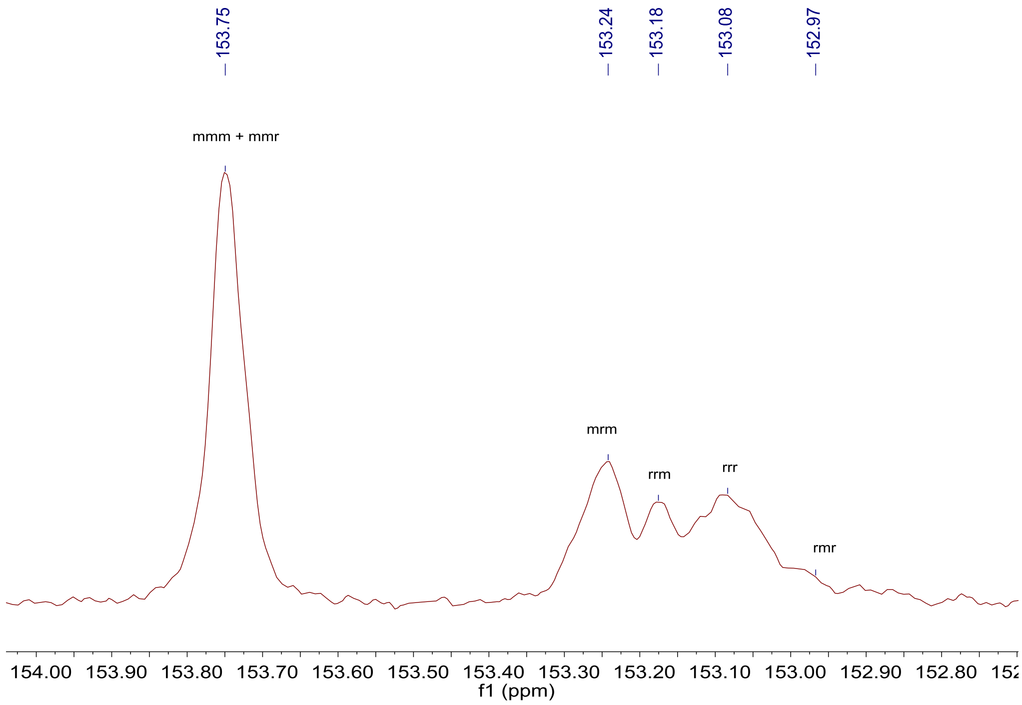

Figure S26 $^{13}C\{^{1}H\}$ NMR spectrum of the poly(cyclohexene carbonate) (Table 1, entry 10) (400 MHz, $CDCl_3$, 25 °C). The spectrum shows only the carbonyl region. Peaks were assigned based on previously reported literature values.[1]

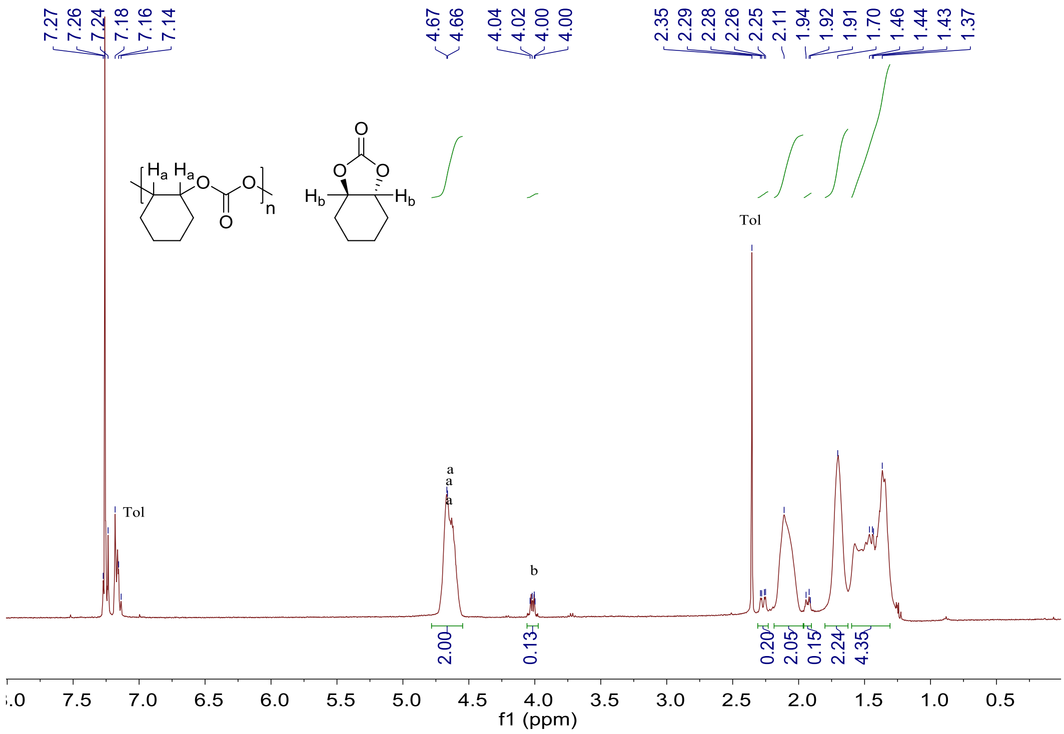

Figure S27 ^{1}H NMR spectra of the poly(cyclohexene carbonate) and cyclic carbonate (Table 1, entry 17) (400 MHz, $CDCl_3$, 25 °C).

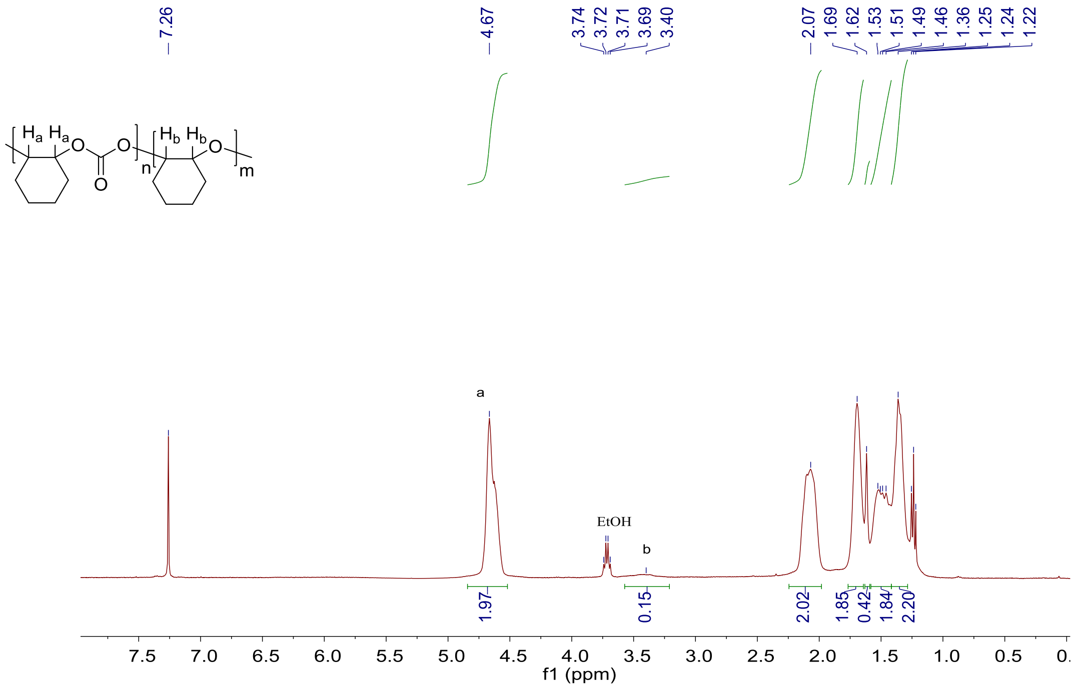

Figure S28 ^{1}H NMR spectra of the poly(cyclohexene carbonate) and polyether (Table 1, entry 1) (400 MHz, $CDCl_3$, 25 °C).

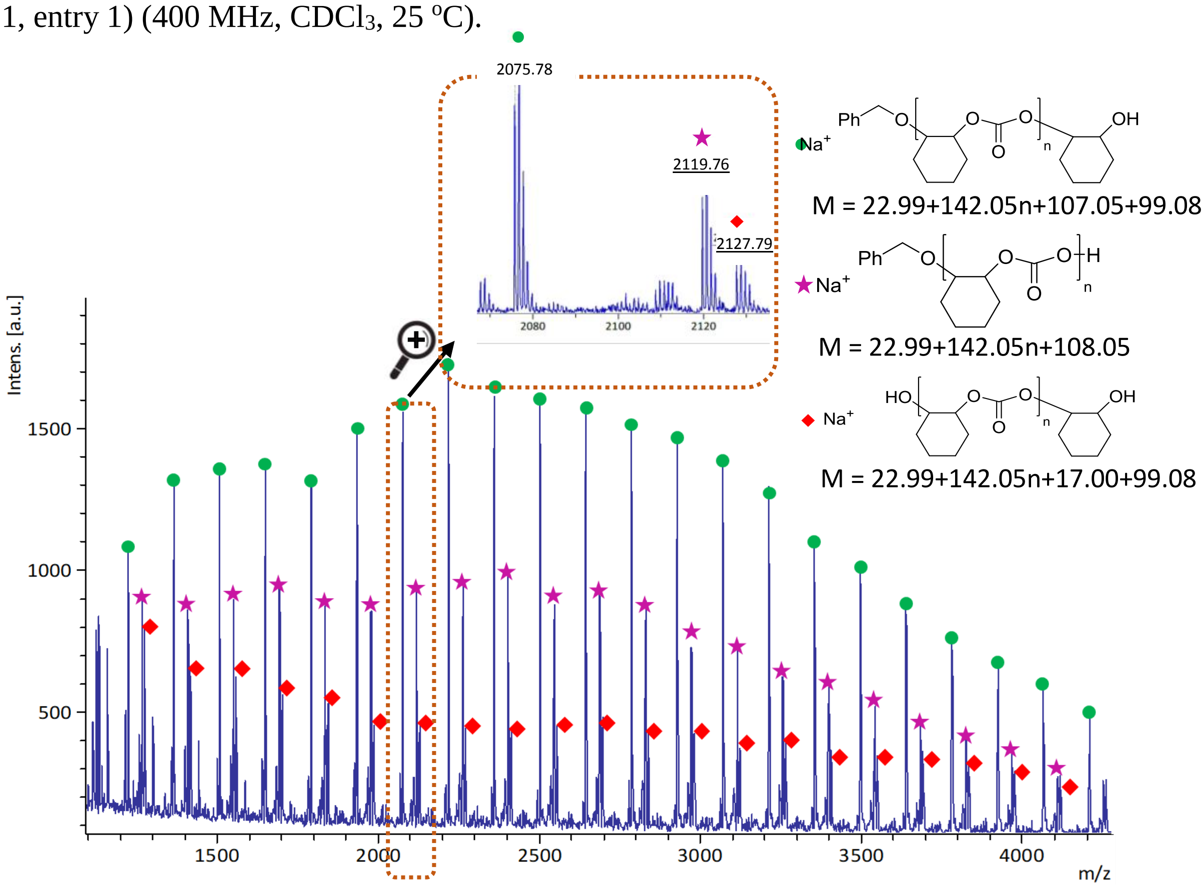

Figure S29 MALDI-TOF mass spectrum of the resultant oligomer. Conditions: V_{tol} = 0.5 mL, V_{CHO} = 1 mL, $[M]_0/[C]_0/[BnOH]$ = 500: 1: 1, T = 70 °C, P_{CO_2} = 1 bar, 12 h.

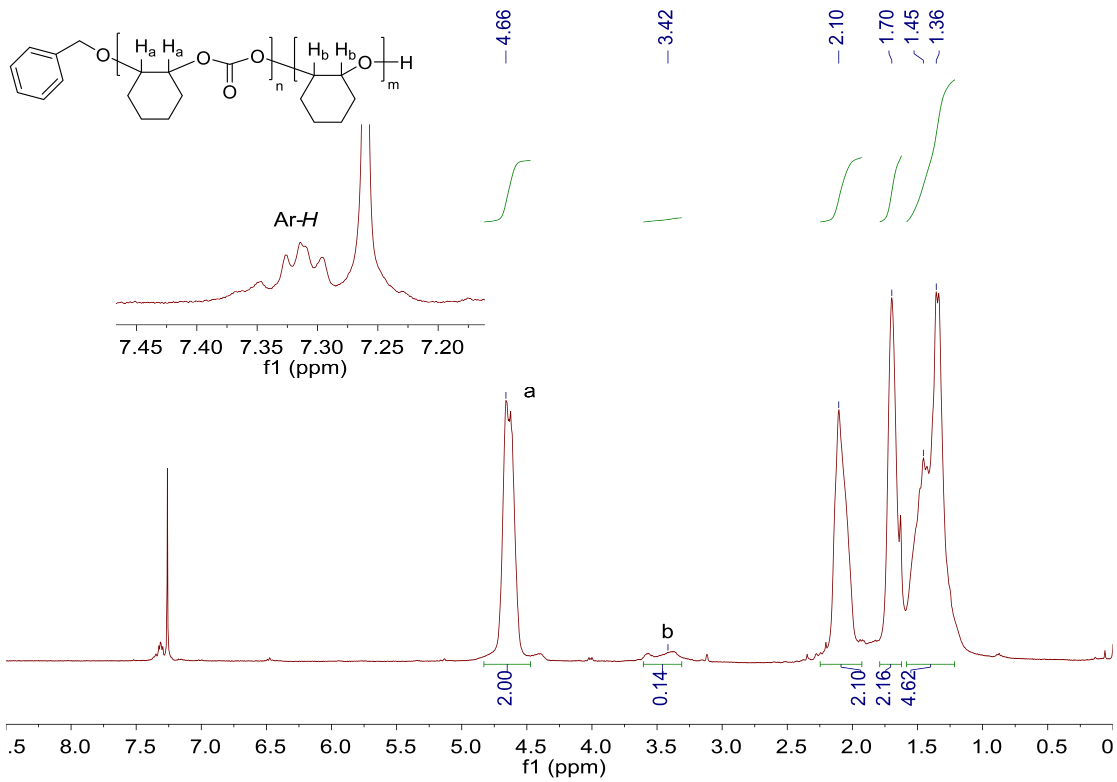

Figure S30 ^{1}H NMR spectra of the poly(cyclohexene carbonate) and polyether (400 MHz, $CDCl_3$, 298K) Conditions: V_{tol} = 0.5 mL, V_{CHO} = 1 mL, $[M]_0/[C]_0/[BnOH]$ = 500: 1: 1, T = 70 °C, P_{CO_2} = 1 bar, 12 h.

References

1. S. Ghosh, D. Pahovnik, U. Kragl and E. Mejía, *Macromolecules*, 2018, **51**, 846–852.